Contents

PART

BASIC PHYSICS

CHAPTER

1

Structure of Matter

1.1. THE ATOM

All matter is composed of individual entities called elements. Each element is distinguishable from the others by the physical and chemical properties of its basic component—the atom. Originally thought to be the "smallest" and "indivisible" particle of matter, the atom is now known to have a substructure and can be "divided" into smaller components. Each atom consists of a small central core, the nucleus, where most of the atomic mass is located and a surrounding "cloud" of electrons moving in orbits around the nucleus. Whereas the radius of the atom (radius of the electronic orbits) is approximately 10^{-10} m, the nucleus has a much smaller radius, namely, about 10^{-15} m.

1.2. THE NUCLEUS

The properties of atoms are derived from the configuration of their nuclei and the number and the organization of the orbital electrons.

The nucleus contains two kinds of fundamental particles: protons and neutrons. Whereas protons are positively charged, neutrons have no charge. Because the electron has a negative *unit charge* (1.602×10^{-19} C) and the proton has a positive unit charge, the number of protons in the nucleus is equal to the number of electrons outside the nucleus of an electrically neutral atom.

An atom is completely specified by the formula ${}^{A}_{Z}X$, where X is the chemical symbol for the element; A is the *mass number*, defined as the number of nucleons (neutrons and protons in the nucleus); and Z is the *atomic number*, denoting the number of protons in the nucleus. An atom represented in such a manner is also called a *nuclide*. For example, ${}^{1}_{1}H$ and ${}^{4}_{2}He$ represent atoms or nuclei or nuclides of hydrogen and helium, respectively.

On the basis of different proportions of neutrons and protons in the nuclei, atoms have been classified into the following categories: *isotopes*, atoms having nuclei with the same number of protons but different number of neutrons; *isotones*, atoms having the same number of neutrons but different number of protons; *isobars*, atoms with the same number of nucleons but different number of protons; and *isomers*, atoms containing the same number of protons as well as neutrons. The last category, namely isomers, represents identical atoms except that they differ in their nuclear energy states. For example, ${}^{131m}_{54}Xe$ (m stands for metastable state) is an isomer of ${}^{131}_{54}Xe$.

Certain combinations of neutrons and protons result in more stable (nonradioactive) nuclides than others. For instance, stable elements in the low atomic number range have an almost

important to point out that the mass of an atom is not exactly equal to the sum of the masses of constituent particles. The reason for this is that, when the nucleus is formed, a certain mass is destroyed and converted into energy that acts as a "glue" to keep the nucleons together. This mass difference is called the *mass defect*. Looking at it from a different perspective, an amount of energy equal to the mass defect must be supplied to separate the nucleus into individual nucleons. Therefore, this energy is also called the *binding energy of the nucleus*.

The basic unit of energy is joule (J) and is equal to the work done when a force of 1 newton acts through a distance of 1 m. The newton, in turn, is a unit of force given by the product of mass (1 kg) and acceleration (1 m/s^2). However, a more convenient energy unit in atomic and nuclear physics is electron volt (eV), defined as the kinetic energy acquired by an electron in passing through a potential difference of 1 V. It can be shown that the work done in this case is given by the product of potential difference and the charge on the electron. Therefore, we have,

$$1 \text{ eV} = 1 \text{ V} \times 1.602 \times 10^{-19} \text{ C} = 1.602 \times 10^{-19} \text{ J}$$

According to Einstein's *principle of equivalence of mass and energy*, a mass m is equivalent to energy E and the relationship is given by

$$E = mc^2 \tag{1.1}$$

where c is the velocity of light (3×10^8 m/s). For example, a mass of 1 kg, if converted to energy, is equivalent to

$$E = 1 \text{ kg} \times (3 \times 10^8 \text{ m/s})^2$$

$$= 9 \times 10^{16} \text{ J} = 5.62 \times 10^{35} \text{ eV}$$

The mass of an electron at rest is sometimes expressed in terms of its energy equivalent (E_0). Because its mass is 9.1×10^{-31} kg, we have from Equation 1.1:

$$E_0 = 5.11 \times 10^5 \text{ eV} = 0.511 \text{ MeV}$$

Another useful conversion is that of u to energy. It can be shown that

$$1 \text{ u} = 931.5 \text{ MeV}$$

From Equation 1.1, we can see that the equivalent mass of any particle of total energy E (kinetic plus rest mass energy) is given by E/c^2. Accordingly, masses of particles may also be expressed in units of GeV/c^2. It can be shown that

$$1 \text{ GeV}/c^2 = 1.0723 \text{ u}$$

In the above examples, we have not considered the effect of particle velocity on its mass. Experiments with high-speed particles have shown that the mass of a particle depends on its velocity and that it increases with velocity. The relationship between mass and velocity can be derived from Einstein's theory of relativity. If m is the mass of a particle moving with velocity v and m_0 is its rest mass, then

$$m = \frac{m_0}{\sqrt{1 - v^2/c^2}} \tag{1.2}$$

The kinetic energy (E_k) is given by

$$E_k = mc^2 - m_0c^2 = m_0c^2 \left[\frac{1}{\sqrt{1 - \frac{v^2}{c^2}}} - 1 \right] \tag{1.3}$$

It should be noted that the relativistic effect of velocity on mass becomes important when a particle travels with a velocity comparable to that of light.

1.4. DISTRIBUTION OF ORBITAL ELECTRONS

According to the model proposed by Niels Bohr in 1913, the electrons revolve around the nucleus in specific orbits and are prevented from leaving the atom by the centripetal force of attraction between the positively charged nucleus and the negatively charged electron.

Figure 6.9. Photographs of the ion chamber and electrometer. **A:** PTW Model TN30013 ion chamber; **B:** CNMC Model 206 electrometer.

6.7. SPECIAL CHAMBERS

A cylindrical thimble chamber is most often used for exposure (or dose) calibration of radiation beams when the dose gradient across the chamber volume is minimal. It is not suitable for surface dose measurements. As will be discussed in Chapters 8 and 13, high-energy photon beams exhibit a *dose buildup* effect, that is, a rapid increase of dose with depth in the first few millimeters. To measure the dose at a point in this buildup region or at the surface, the detector must be very thin along the direction of the beam so that there is no dose gradient across its sensitive volume. In addition, the chamber cavity must not significantly perturb the radiation field. Special chambers have been designed to achieve the above requirements.

A. EXTRAPOLATION CHAMBER

Failla (8) designed an ionization chamber for measuring surface dose in an irradiated phantom in 1937. He called this chamber an extrapolation chamber (Fig. 6.10). The beam enters through a thin foil window that is carbon coated on the inside to form the upper electrode. The lower or the collecting electrode is a small disk-shaped region surrounded by a guard ring and is connected to an electrometer. The electrode spacing can be varied accurately by micrometer screws. By measuring the ionization per unit volume as a function of electrode spacing, one can estimate the incident dose by extrapolating the ionization curves to zero electrode spacing.

The extrapolation chambers of the type described earlier have been used for special dosimetry (e.g., the measurement of dose in the superficial layers of a medium and the dosimetry of electrons and β particles).

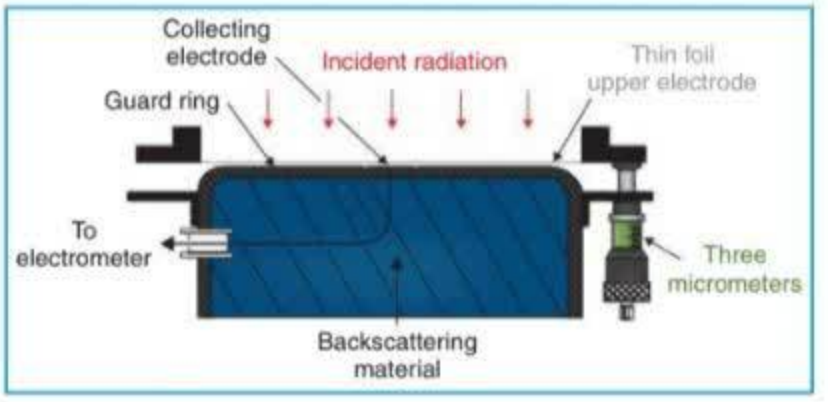

Figure 6.10. Extrapolation ion chamber by Failla. (Redrawn from Boag JW. Ionization chambers. In: Attix FH, Roesch WC, eds. *Radiation Dosimetry*. Vol 2. New York, NY: Academic Press; 1969:1.)

TABLE 8.2 k_Q Values for Accelerator Photon Beams as a Function of %dd(10)$_x$ for Cylindrical Ion Chambers

	k_Q				
	%dd(10)$_x$				
Ion Chamber	**63.0**	**67.0**	**73.0**	**77.0**	**81.0**
Capintec PR-06C/G	0.998	0.993	0.985	0.979	0.971
Exradin A19	0.996	0.991	0.981	0.974	0.966
Exradin A12	0.997	0.992	0.983	0.976	0.968
Exradin A12S	0.996	0.992	0.983	0.976	0.968
Exradin A18	0.997	0.992	0.983	0.976	0.969
Exradin A1	0.996	0.991	0.981	0.975	0.967
Exradin A1SL	0.997	0.992	0.983	0.977	0.969
NE NE2561	0.999	0.994	0.985	0.978	0.971
NE NE2571	0.997	0.992	0.983	0.976	0.968
PTW N30010	0.997	0.992	0.983	0.976	0.968
PTW N30011	0.997	0.992	0.983	0.976	0.969
PTW N30012	0.998	0.994	0.985	0.979	0.971
PTW N30013	0.996	0.991	0.982	0.975	0.967
PTW N31013	0.997	0.992	0.982	0.975	0.967
IBA FC65-G	0.997	0.992	0.983	0.976	0.968
IBA FC65-P	0.997	0.991	0.982	0.975	0.967
IBA FC23-C	0.996	0.991	0.982	0.975	0.968
IBA CC25	0.997	0.992	0.984	0.977	0.969
IBA CC13	0.996	0.992	0.983	0.976	0.969
IBA CC08	0.995	0.990	0.982	0.975	0.967

For ^{60}Co beams, $k_Q = 1.000$ by definition.

From McEwen M, DeWerd L, Ibbott G, et al. Addendum to the AAPM TG-51 protocol for clinical reference dosimetry of high-energy photon. *Med Phys.* 2014;41:041501, with permission.

The updated k_Q values are very close (within 0.5%) to those originally published in TG-51. Data for plane-parallel chambers are not included because of insufficient information about P_{wall} in photon beams, other than ^{60}Co for which $k_Q = 1$ by definition for all chambers.

B.2. k_Q for Electron Beams

Although Equation 8.47 is general and can be applied for both photon and electron beams (see IAEA protocol, Section 8.7), the authors of the TG-51 protocol felt that for electron beams the P_{gr}^{Q} factor in Equation 8.57 at the reference point of measurement may vary from one accelerator to another and therefore must be measured in the user's beam. Thus, k_Q has been redefined for electron beams by the following equations (34):

$$k_Q = P_{gr}^{Q} k_{R_{50}} \tag{8.58}$$

where

$$k_{R_{50}} = \frac{\left[\left(\bar{L}/\rho\right)_{air}^{w} P_{wall} P_{fl} P_{cel}\right]_Q}{\left[\left(\bar{L}/\rho\right)_{air}^{w} P_{wall} P_{fl} P_{cel}\right]_{60_{Co}}} \tag{8.59}$$

and P_{gr}^{Q} is the gradient correction at the reference depth of measurement. The reference depth, called d_{ref}, for electron beams is based on recommendations by Burns et al. (35) and is given by

$$d_{ref} = 0.6\, R_{50} - 0.1 \tag{8.60}$$

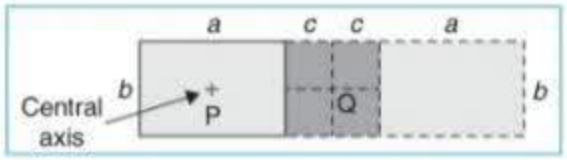

Figure 10.11. Calculation of depth dose outside a rectangular field. (See text.)

For higher-energy beams (≥8 MV), the above procedure may be further simplified by assuming BSF = 1 for all field sizes. Also, Day's procedure can be adopted using S_p values instead of BSF, because the two quantities are related by Equation 10.1.

C. POINT OUTSIDE THE FIELD

Day's method can be extended also to the case of determining dose distribution at points outside the field limits. In Figure 10.11, a rectangular field of dimensions $a \times b$ is shown, with the central axis passing through P. Suppose Q is a point outside the field at a distance c from the field border. Imagine a rectangle adjacent to the field such that it contains point Q and has dimensions $2c \times b$. Place another rectangle of dimensions $a \times b$ on the other side of Q such that the field on the right of Q is a mirror image of the field on the left, as shown in the figure. The dose at point Q at depth d is then given by subtracting the depth dose at Q for field $2c \times b$ from that for field $(2a + 2c) \times b$ and dividing by 2. The procedure is illustrated by the following example.

Example 7

Suppose it is required to determine PDD at Q (relative to D_{max} at P) outside a 15 × 10-cm field at a distance of 5 cm from the field border. In Figure 10.11, then, $a = 15$, $b = 10$, and $c = 5$. Suppose Q is at the center of the middle rectangle of dimensions $2c \times b$. Then, the dose D_Q at 10 cm depth is given by

$$\frac{1}{2}\left[D_Q(40\times10) - D_Q(10\times10)\right]$$

If D_Q is normalized to D_{max} at P, one gets the PDD at Q or $\%D_Q$.

$$\%D_Q = \frac{1}{\text{BSF}(15\times10)} \cdot \frac{1}{2}[\text{BSF}(40\times10)\times\%\text{DD}(40\times10) - \text{BSF}(10\times10)\times\%\text{DD}(10\times10)]$$

Thus, for a ^{60}Co beam at SSD = 80 cm,

$$\%D_Q = \frac{1}{1.043} \cdot \frac{1}{2}[1.054\times58.8 - 1.036\times55.6] = 9.1$$

Again, for higher-energy beams, the above procedure is simplified by assuming BSF = 1. Also, if S_p values are known instead of BSF, the above calculation can be performed by substituting S_p for BSF.

D. POINT UNDER THE BLOCK

As discussed earlier, the dose distribution in a blocked field is best determined by Clarkson's method of irregular field dosimetry. However, if the blocked portion of the field is approximated to a rectangle, a simpler method known as negative field method may be used. The concept of negative field has been described in the literature (26,27). In this method, the dose at any point is equal to the dose from the overall (unblocked) field minus the dose expected if the entire field were blocked, leaving the shielded volume open. In other words, the blocked portion of the field is considered a negative field and its contribution is subtracted from the overall field dose distribution.

A computerized negative field method not only is a fast method of calculating isodose distribution in blocked fields, but is also very convenient for manual point dose calculation. Its practical usefulness is illustrated by Example 8.

Example 8

A patient is treated with a split field of overall size 15 × 15 cm^2, blocked in the middle to shield a region of size 4 × 15 cm^2 on the surface (Fig. 10.12). Calculate (a) the treatment time to deliver 200 cGy at a 10-cm depth at point P in the open portion of the field and (b) what percentage of that dose is received at point Q in the middle of the blocked area, given ^{60}Co beam, SSD = 80 cm,

Figure 12.8. Ultrasonic tomogram showing chest wall thickness **(right)** compared with the computed tomography image **(left)**.

signal from a point in the medium is displayed by an echo dot on the CRT. The (x, y) position of the dot on the CRT indicates the location of the reflecting point at the interface and its proportional brightness reveals the amplitude of the echo. By scanning across the patient, the B-mode viewer sees an apparent cross section through the patient. Such cross-sectional images are called *ultrasonic tomograms*.

In the M mode of presentation, the ultrasound images display the motion of internal structures of the patient's anatomy. The most frequent application of M-mode scanning is echocardiography. In radiotherapy, the cross-sectional information used for treatment planning is exclusively derived from the B-scan images (Fig. 12.8).

12.2. TREATMENT SIMULATION

A. RADIOGRAPHIC SIMULATOR

Treatment simulator (Fig. 12.9) is an apparatus that uses a diagnostic x-ray tube but duplicates a radiation treatment unit in terms of its geometric, mechanical, and optical properties. The main function of a simulator is to display the treatment fields so that the target volume may

Figure 12.9. **A:** Photograph of Varian Ximatron CDX simulator at the University of Minnesota. **B:** Varian Acuity simulator that has superseded the Ximatron. (Courtesy of Varian Associates, Palo Alto, CA.)

CHAPTER

15 Low-Dose-Rate Brachytherapy: Rules of Implantation and Dose Specification

Brachytherapy is a method of treatment in which sealed radioactive sources are used to deliver radiation at a short distance by interstitial, intracavitary, or surface application. With this mode of therapy, a high radiation dose can be delivered locally to the tumor with rapid dose falloff in the surrounding normal tissue. In the past, brachytherapy was carried out mostly with radium or radon sources. Currently, use of artificially produced radionuclides such as ^{137}Cs, ^{192}Ir, ^{198}Au, ^{125}I, and ^{103}Pd is more common.

Technical developments in the last few decades have stimulated increased interest in brachytherapy: the introduction of low-energy sources, afterloading devices to reduce personnel exposure, and automatic devices with remote control to deliver controlled radiation exposure from high-activity sources. Although electrons are often used as an alternative to interstitial implants, brachytherapy continues to remain an important mode of therapy, either alone or combined with external beam.

15.1. RADIOACTIVE SOURCES

From the time of its discovery in 1898, radium has been the most commonly used isotope in brachytherapy. However, artificial radioisotopes offer special advantages in some situations because of their γ-ray energy, source flexibility, source size, and half-life. Table 15.1 lists some of the brachytherapy sources that have been or are currently being used with their relevant physical properties.

A. RADIUM

Although radium is no longer clinically used in brachytherapy, the physics of this source is discussed here for historic interest. Also, vast amounts of clinical data pertaining to radium therapy exist in the literature, which are often used by clinicians to compare treatment outcomes and dosage specification in modern brachytherapy.

A.1. Decay

Radium is the sixth member of the uranium series, which starts with $^{238}_{92}$U and ends with stable $^{206}_{82}$Pb (Fig. 2.3). Radium disintegrates with a half-life of about 1,600 years to form radon:

$$^{226}_{88}\text{Ra} \xrightarrow[\sim 1{,}600\,\text{years}]{} {}^{222}_{86}\text{Rn} + {}^{4}_{2}\text{He}$$

The product nucleus radon is a heavy inert gas that in turn disintegrates into its daughter products as shown in Figure 2.3. As a result of the decay process from radium to stable lead, at least 49 γ-rays are produced with energies ranging from 0.184 to 2.45 MeV. The average energy of the γ-rays from radium in equilibrium with its daughter products and filtered by 0.5 mm of platinum is 0.83 MeV (1). A filtration of at least 0.5 mm platinum provided by the source case is sufficient to absorb all α particles and most of the β particles emitted by radium and its daughter products. Only γ-rays are used for therapy.

C. IMAGE SEGMENTATION

The term *image segmentation* in treatment planning refers to slice-by-slice delineation of anatomic regions of interest, for example, external contours, targets, critical normal structures, and anatomic landmarks. The segmented regions can be rendered in different colors and can be viewed in BEV configuration or in other planes using DRRs. Segmentation is also essential for calculating DVHs for the selected regions of interest.

Image segmentation is one of the most laborious but important processes in treatment planning. Although the process can be aided for automatic delineation based on image contrast near the boundaries of structures, target delineation requires clinical judgment, which cannot be automated or completely image based. Nor should it be delegated to personnel other than the physician in charge of the case, the radiation oncologist. Figure 19.3 shows an example of a segmented image for prostate gland treatment planning.

D. BEAM APERTURE DESIGN

After image segmentation has been completed, the treatment planner gets to the task of selecting beam directions and designing beam apertures. This is greatly aided by the BEV capability of the 3-D treatment-planning system. Targets and critical normal structures made visible through segmentation can be viewed from different directions in planes perpendicular to the beam's central axis. Beam directions that create greater separation between targets and critical structures are generally preferred, unless other constraints such as obstructions in the path of the beam and gantry collision with the couch or patient preclude those choices. BEV capability, combined with DRRs, is a powerful tool in selecting beam directions and shaping fields around the target.

Beam apertures can be designed automatically or manually depending on the proximity of the critical structures and the uncertainty involved in the allowed margins between the CTV and PTV. Depending on the planning software, users may set uniform or nonuniform margins around the PTV, either manually or automatically. A considerable give and take occurs between target coverage and sparing of critical structures in cases where the spaces between the target and critical structures are tight, thus requiring manual design of the beam apertures. In simpler cases, automatic margins may be assigned between the PTV and field edges, taking into

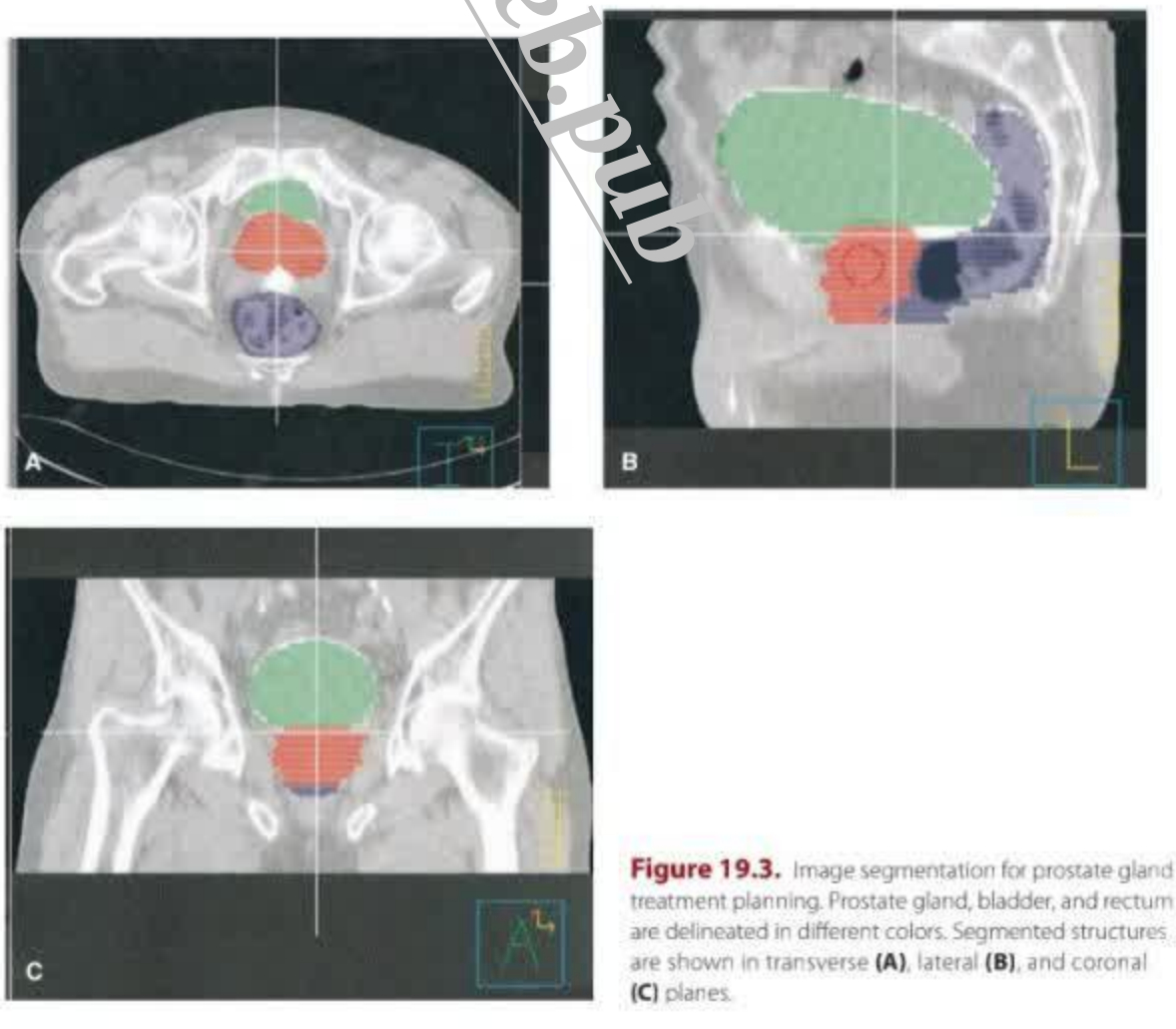

Figure 19.3. Image segmentation for prostate gland treatment planning. Prostate gland, bladder, and rectum are delineated in different colors. Segmented structures are shown in transverse **(A)**, lateral **(B)**, and coronal **(C)** planes.

certain parts of the target, usually the GTV), a composite isodose plan is useful, which can again be displayed by isodose distribution in individual slices, in orthogonal planes, or as isodose surfaces.

F.2. Dose-Volume Histograms

Display of dose distribution in the form of isodose curves or surfaces is useful because it shows not only regions of uniform dose, high dose, or low dose, but also their anatomic location and extent. In 3-D treatment planning, this information is essential but should be supplemented by DVHs for the segmented structures, for example, targets and critical structures. A DVH not only provides quantitative information with regard to how much dose is absorbed in how much volume, but also summarizes the entire dose distribution into a single curve for each anatomic structure of interest. It is, therefore, a great tool for evaluating a given plan or comparing competing plans.

The DVH may be represented in two forms: the cumulative integral DVH and the differential DVH. The cumulative DVH is a plot of the volume of a given structure receiving a *certain dose or higher* as a function of dose (Fig. 19.6). Any point on the cumulative DVH curve shows the volume that receives the indicated dose or higher. The differential DVH is a plot of volume receiving a dose within a specified dose interval (or dose bin) as a function of dose. As seen in Figure 19.6 E, the differential form of DVH shows the extent of dose variation within a given structure. For example, the differential DVH of a uniformly irradiated structure is a single bar of 100% volume at the stated dose. Of the two forms of DVH, the cumulative DVH has been found to be more useful and is more commonly used than the differential form.

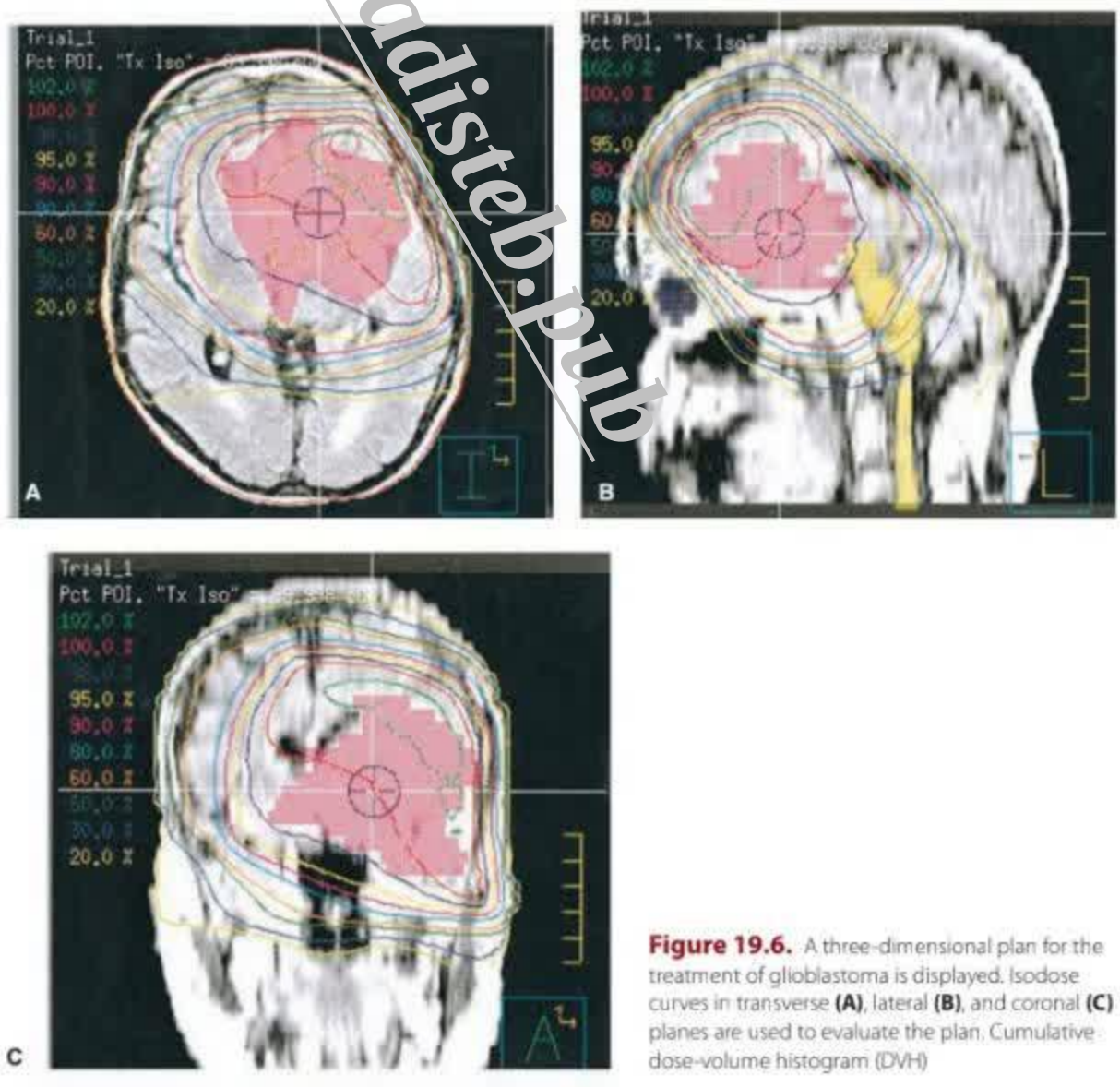

Figure 19.6. A three-dimensional plan for the treatment of glioblastoma is displayed. Isodose curves in transverse **(A)**, lateral **(B)**, and coronal **(C)** planes are used to evaluate the plan. Cumulative dose-volume histogram (DVH)